© Volume 2, Issue 8, ***August*** 2026 | JATIR
ISSN: 3139-8464 (p)

Monte Carlo-Optimized Tensile Strength and Stiffness of Mapp-Enhanced Polypropylene (PP)/Palm Kernel Shell Powder (PKSP) Bio Composites for Rigid Food Packaging Application

[1]P.A. Mbah, [2]E.C Oriaku, [3]U.O Udeh, [4]A.E. Esuvbie
[1]Engineering Research Development & Production, Projects Development Institute (PRODA) Emene-Enugu, Nigeria
[2,3]Department of Mechanical Engineering, Caritas University Amorji-Nike Enugu, Nigeria
[4]Material & Energy Technology Department, Projects Development Institute (PRODA), Emene Enugu, Nigeria

***Abstract*—The pressing environmental challenges posed by conventional petroleum-derived plastics have accelerated the exploration of sustainable alternatives, particularly biocomposites derived from agricultural waste. This investigation focuses on the development and performance optimization of a rigid biocomposite material composed of polypropylene (PP) reinforced with palm kernel shell powder (PKSP) a readily available lignocellulosic byproduct of the palm oil industry. The target application is rigid food service and packaging products such as plates, trays, cups, containers, and lids. PKSP underwent comprehensive characterization prior to composite fabrication with maleic anhydride-grafted polypropylene (MAPP) enhanced PP. Composite specimens measuring 15 mm × 15 mm × 100 mm were produced through melt mixing followed by compression molding, with PKSP concentrations ranging from 5 wt% to 25 wt% across three particle size fractions: 75 µm, 250 µm, and 500 µm. Tensile properties, specifically strength and modulus, were rigorously assessed using an electronic Universal Testing Machine (UTM-YYL016) in accordance with ASTM protocols. Monte Carlo optimization algorithms, executed through custom Python programming, were subsequently applied to identify the optimal particle size and loading combinations that maximize mechanical performance. The analysis yielded three distinct optimized formulations: (75 µm, 25 wt%) offering the most favorable strength-stiffness balance at 166.77 MPa·GPa; (75 µm, 5 wt%) exhibiting peak tensile strength of 35.60 MPa; and (500 µm, 25 wt%) demonstrating maximum tensile stiffness of 5.64 GPa.**

Experimental outcomes reveal that PKSP incorporation markedly improves composite stiffness, accompanied by a modest, acceptable decline in tensile strength a characteristic behavior in particulate-filled systems. These findings substantiate PKSP as an economically viable, environmentally sustainable reinforcing agent for polypropylene, thereby confirming its practical applicability in rigid food packaging. This work contributes meaningfully to agricultural residue valorization, fosters circular economic models, and promotes the advancement of eco-friendly polymeric materials for packaging applications.

Index Terms—**Polypropylene (PP), palm kernel shell powder (PKSP), Maleic Anhydride-grafted Polypropylene (MAPP), bio-composite, natural filler, mechanical properties, compatibilizer, compression molding, optimization, sustainable materials, food packaging, waste Valorization, greener materials.**

I. INTRODUCTION

Growing anxieties over the environmental toll exacted by the widespread utilization of petroleum-derived plastics have catalyzed an intensification of research efforts directed toward sustainable material alternatives, with the food packaging sector emerging as a primary focal point [11]. Although traditional plastic packaging materials demonstrate commendable mechanical robustness and effective barrier characteristics, they pose considerable ecological threats owing to their reliance on finite fossil resources and their resistance to natural degradation processes [11]. The accumulation of plastic refuse substantially compounds environmental deterioration, as enormous quantities of packaging waste ultimately find their way into landfills and natural ecosystems [11]. The challenges associated with managing plastic waste at the conclusion of its useful life, coupled with escalating production rates and increasingly brief utilization windows, have emerged as pressing concerns necessitating prompt remedial action [19]. This heightened awareness regarding plastic pollution has stimulated substantial interest in the creation of packaging materials derived from renewable biological resources that offer enhanced environmental compatibility [19].

Natural fiber-reinforced polymer composites (NFRPCs) have positioned themselves as attractive substitutes for traditional synthetic materials, affording the simultaneous advantages of diminished ecological footprint and superior material characteristics [8]. These bio-based composites constitute a distinctive category of materials produced through the combination of a polymeric matrix with natural fiber reinforcements, capitalizing on the inherent biodegradability and adaptable attributes of natural fibers whilst preserving the desirable processing characteristics of thermoplastic polymers [15]. Contemporary scholarly assessments have thoroughly catalogued the promise exhibited by diverse natural fibers among them jute, sisal, hemp, bamboo, and kenaf as environmentally responsible reinforcing agents suitable for composite fabrication and packaging applications [12]. Lignocellulosic fibers have drawn considerable research attention owing to their modest density, minimal abrasive tendencies, and favorable inherent mechanical attributes [12]. Additionally, the reprocessing and repurposing of agricultural byproducts into composite materials

serves the dual purpose of reducing material costs and advancing sustainability objectives and circular economic frameworks [17].

Within the extensive array of agricultural residual materials amenable to composite reinforcement, palm kernel shell (PKS) has attracted noteworthy scholarly interest as a particularly advantageous filler candidate [5]. PKS represents an abundant secondary product arising from the conversion of palm kernels into edible oil, offering an economical, lightweight, and renewable substitute for traditional inorganic fillers including basalt, graphite, mica, and aluminum magnesium silicate [1]. The deployment of PKS as a reinforcing agent simultaneously addresses two pressing sustainability imperatives: the beneficial repurposing of agricultural discards and the diminished dependence on exhaustible mineral resources [17].

Prior scholarly investigations concerning PKS-reinforced polypropylene (PP) composites have laid essential groundwork concerning their mechanical response characteristics [9]. Experimental evidence indicates that the introduction of PKS as a filler typically produces enhanced tensile and flexural moduli within the PP matrix, although these improvements are frequently accompanied by diminished tensile strength, flexural strength, and elongation at fracture [1]. Systematic studies have documented decreases in tensile strength, flexural strength, and elongation at break corresponding to incremental increases in filler concentration, whilst tensile modulus, flexural modulus, and moisture uptake exhibited upward trends [17]. Microscopic examination employing scanning electron microscopy (SEM) has disclosed inadequate interfacial bonding between PKS particulates and the PP matrix as filler content escalates, attributable to the fundamental incompatibility existing between hydrophilic lignocellulosic materials and hydrophobic polymeric matrices [9]. This interfacial deficiency constitutes a primary obstacle in the advancement of natural fiber composite technologies [7]. The influence of filler particle dimensions on composite performance characteristics has likewise been scrutinized, with findings indicating that micro-scale filler systems exhibit superior tensile strength under conditions of optimized filler loading [20]. Furthermore, investigations into composites incorporating diverse agricultural waste fillers have verified that materials containing agro-waste components display enhanced stiffness relative to unmodified PP matrices achieving improvements of up to 49% alongside elevated tensile strength, though these gains are realized at the expense of reduced ductility [17].

Various compatibilization methodologies have been investigated as potential solutions to the interfacial adhesion difficulties inherent in natural fiber composites [7]. Maleic anhydride-grafted polypropylene (MAPP) has established itself as one of the most efficacious coupling agents for promoting compatibility between natural fillers and PP matrices [9]. The maleic anhydride functional groups present in MAPP establish hydrogen bonds with hydroxyl moieties situated on the natural filler surface, whilst the polypropylene backbone maintains compatibility with the PP matrix, thereby forming covalent connections that strengthen interfacial bonding [7].

Research findings consistently affirm that MAPP incorporation substantially improves the mechanical performance of natural fiber-reinforced PP composites [9]. In particular, PP-g-MAH compatibilizer has been demonstrated to confer superior tensile strength relative to uncompatibilized biocomposites, with additional evidence indicating concurrent enhancements in

tensile strength and elongation at break upon compatibilizer addition [9]. PP-g-MAH also contributed to elevated Young's modulus values in the biocomposite systems under investigation [9]. Furthermore, the inclusion of compatibilizing agents resulted in diminished water absorption characteristics [9]. These compatibilizers augmented the nucleating capability of fillers within the composite structure, with PP-g-MAH demonstrating particular effectiveness in this regard relative to alternative compatibilizer types [7]. Investigation of curaua/polypropylene composite systems revealed that optimal tensile strength was achieved at a MAPP-to-fiber proportion of 6 wt%, identified as the optimum concentration owing to the restricted availability of reactive hydroxyl groups located on the external fiber surface layers [18]. Chemical treatment of PP/PKS biocomposites employing coupling agents has been shown to produce improvements in tensile strength, tensile modulus, flexural strength, flexural modulus, and crystallinity, accompanied by diminished water absorption capabilities [2]. Morphological examinations have confirmed enhanced filler-matrix interaction following chemical modification procedures [2].

Although the advantageous effects of PKS incorporation and MAPP compatibilization have been qualitatively confirmed, the methodical optimization of processing parameters and formulation variables continues to represent a significant research requirement [1]. Prior investigations have generally depended on conventional trial-and-error methodologies to ascertain appropriate filler loadings and particle dimensions [9]. Nevertheless, these approaches may inadequately address the intricate, interactive relationships existing among multiple formulation variables and their collective influence on composite mechanical behavior [6].

Contemporary developments in computational materials science have introduced advanced optimization strategies, incorporating Monte Carlo simulation methodologies, for the systematic engineering and optimization of polymer composites [6]. Monte Carlo approaches, executed through computational algorithms, facilitate the efficient examination of extensive parameter spaces and the identification of optimal combinations that effectively reconcile competing performance requirements [6]. Scholarly work has established that Gaussian process regression in conjunction with Monte Carlo sampling across randomized iterations can successfully represent nonlinear relationships and uncertainty propagation within datasets, surpassing the performance of conventional models including support vector machines, regression trees, and artificial neural networks [6]. These computationally driven methodologies facilitate informed material design and optimization processes, particularly under conditions of limited data availability [6]. Sensitivity analyses have identified filler weight fraction, matrix tensile strength, and surface modification approaches as the predominant factors affecting predictive accuracy [6].

Notwithstanding the expanding body of literature addressing PKS-reinforced PP composites, several knowledge gaps persist within the existing scholarly record [1, 9]. Firstly, although the consequences of filler loading on mechanical properties have been examined, the combined influence of particle size and filler concentration on tensile performance has yet to be comprehensively optimized through advanced computational techniques [6]. Secondly, the particular application of these materials to rigid food packaging encompassing plates, cups, trays, containers, and lids necessitates a customized optimization strategy that effectively reconciles

strength and stiffness requirements to ensure structural integrity during service [17]. Thirdly, the identification of optimal formulation parameters capable of simultaneously maximizing diverse mechanical performance indicators namely strength, stiffness, and their equilibrium has not been methodically addressed [6].

Consequently, the principal aim of this research endeavor is the development and optimization of a rigid biocomposite material formulation possessing enhanced mechanical characteristics, specifically engineered for rigid food service and packaging applications [16]. Palm kernel shell powder (PKSP) undergoes comprehensive characterization, and MAPP-enhanced PP/PKSP composites are fabricated through melt blending followed by compression molding [1]. Tensile strength and tensile stiffness are methodically assessed in accordance with ASTM protocols across a range of PKSP concentrations (5 wt% to 25 wt%) and particle size fractions (75 µm, 250 µm, and 500 µm) [9]. Monte Carlo optimization algorithms, implemented via Python programming scripts, are subsequently applied to numerically ascertain the optimal particle size and loading combinations that yield the most favorable balance of strength and stiffness, maximum overall strength, and maximum overall stiffness [6]. This investigation contributes to the overarching objectives of agricultural waste valorization, advancement of circular economic principles, and development of environmentally preferable polymeric materials for packaging applications [17], thereby addressing the urgent environmental necessity to supplant conventional petroleum-derived plastics with sustainable alternatives [4, 8, 11].

II. MATERIALS AND METHODS

Collection of Materials

Maleic anhydride-grafted polypropylene (MAPP), sourced from Indorama Eleme Petrochemicals Limited (IEPL), Port Harcourt, was dried at 90 °C for 10 hours to remove residual moisture before further processing. Palm kernel shells (PKS), obtained from Aniuzo Oil (Emene Industrial Layout, Enugu), were cleaned, dried, milled, and sieved into 75 µm, 250 µm, and 500 µm fractions. Prior to processing, the sieved PKS (PKSP) underwent partial carbonization at 300 °C to drive off moisture and light volatiles without fully degrading the biomass structure thereby yielding a carbon-rich solid.

Design of Experiments (DOE)

A Python script for Monte Carlo–based Design of Experiments (DOE) was applied to model the tensile strength and stiffness of MAPP-enhanced polypropylene filled with partially oxidized PKSP, considering 3 particle sizes and 5 filler loadings. While the full factorial design comprises 15 experiments, the Monte Carlo optimization can selectively prioritize or augment these combinations.

Mathematical Formulation

A Monte Carlo mathematical formula for polymer composite optimization was used for the design calculation.

ISSN: 3139-8464 (p)

Let the design vector be

$$\mathbf{X} = [x_1, x_2, x_3, \ldots, x_n]$$

where

- x_1 = Particle size (µm)
- x_2 = Filler loading (wt%)
- x_3 = MAPP content (wt%)
- x_4 = Processing temperature (optional)
- x_5 = Screw speed (optional)

Each variable is sampled from a uniform distribution within its experimental limits:

$$x_i \sim U(x_{i,\min}, x_{i,\max})$$

The response is predicted using the quadratic response surface model:

$$\hat{Y} = \beta_0 + \sum_{i=1}^{n} \beta_i X_i + \sum_{i=1}^{n} \beta_{ii} X_i^2 + \sum_{i<j}^{n} \beta_{ij} X_i X_j$$

The Monte Carlo optimization searches for the design vector that maximizes (or minimizes) the objective:

$$\mathbf{X}^* = \arg\max_{\mathbf{X} \in \Omega} \hat{Y}(\mathbf{X})$$

where Ω is the feasible design space defined by the variable bounds.

For multi-response optimization (e.g., maximizing tensile strength, tensile modulus, flexural strength, and impact strength simultaneously), a composite objective such as the geometric mean or desirability function can be used:

$$D = \left(\prod_{i=1}^{m} d_i \right)^{1/m}$$

where d_i is the individual desirability of the i-th response and m is the number of responses. The optimal formulation is obtained by maximizing the overall desirability:

$$\mathbf{X}^* = \arg\max_{\mathbf{X} \in \Omega} D(\mathbf{X})$$

Experimental Design Framework

Table 1: Experimental Design Framework

Factor	Levels	Rationale
PKSP Particle Size	75, 250, 500 µm	Three distinct sizes to evaluate the effect of filler fineness on mechanical properties
Filler Loading	0, 5, 10, 15, 20, 25 wt%	Five loading levels and neat MAPP - enhanced PP (0 wt.%) as a control baseline

ISSN: 3139-8464 (p)

Composite formulation

MAPP-enhanced PP was selected over neat homopolymer PP to promote superior interfacial adhesion with the PKSP filler. This improved binding minimizes voids and interfacial defects, thereby maximizing both the tensile strength and stiffness of the composite. Furthermore, the PKSP was lightly carbonized in a Carbolyte-300 carbonizer to moderately elevate its carbon content which enhances matrix rigidity and stiffness while preserving sufficient O– and OH– groups to ensure strong MAPP-mediated bonding and retain tensile strength. As a result, this partially carbonized filler yields a composite that is significantly stiffer than one containing raw PKSP, yet avoids the strength loss typically associated with fully carbonized PKSP.

Composite plaques were subsequently prepared according to the formulations outlined in Table 2, with PKSP loadings ranging from 0 to 25 wt%.

Table 2: Composite Matrix Formulation

Formulation Code	PKSP Size (μm)	PKSP (wt%)	MAPP-enhanced PP (wt%)
PP-0	0	0	100
S75-L5	75	5	95
S75-L10	75	10	90
S75-L15	75	15	85
S75-L20	75	20	80
S75-L25	75	25	75
S250-L5	250	5	95
S250-L10	250	10	90
S250-L15	250	15	85
S250-L20	250	20	80
S250-L25	250	25	75
S500-L5	500	5	95
S500-L10	500	10	90
S500-L15	500	15	85
S500-L20	500	20	80
S500-L25	500	25	75

Composite fabrication

The fabrication process consisted of the following steps:

1. Drying:

The MAPP-enhanced PP pellets and slightly carbonized PKSP filler were dried at 90°C for 10 hours to removed absorbed moisture, which could otherwise cause voids during measurement and melt processing.

ISSN: 3139-8464 (p)

2. Weighing:
The required amount of MAPP- enhanced PP and slightly carbonized PKSP were accurately weighed using a digital balance with a precision of ± 0.01 g, according to the formulation in Table 3.1. the total batch weight for each formulation was kept constant at 500g to maintain consistent processing conditions.

3. Pre-mixing (Dry Blending):
The weighed MAPP-enhanced PP and the partially carbonized PKSP fillers were initially dry-mixed manually in a high-speed laboratory blender at room temperature for 5 minutes at 1000 rpm. This set ensures a preliminary homogenous distribution of the PKSP particulates within the PP matrix before melt processing according to the specified formulations.

4. Melt compounding:
The mixtures were melt-blended using a twin-screw extruder at a temperature profile of 170-185°C from the speed zone to the die with a screw speed of 60 rpm. The mixture was compounded for 10 minutes to achieve uniform dispersion of the PKSP particles within the molten PP matrix for each composite formulation.

5. Molding:
The different compounded mixtures were placed into a square shaped mold cavity (dimension of 15 mm x 15 mm x 100 mm) that was preheated to 180°C. The compounded mixture was properly pressed inside the mold and was held for 5 minutes to allow the materials to fully fill the mold cavity and eliminate internal voids.

6. Cooling:
The mold was then cooled to room temperature under pressure using a water circulating cooling system for 4 hours at a rate of approximately 10℃/mm to prevent thermal shrinkage and warpage.

7. Demolding:
After cooling, the solidified square composites rods were carefully removed from the mold.

Characterization and Testing.
Tensile properties (strength and stiffness) of the molded composites were evaluated per ASTM standards using an electronic universal testing machine (UTM). A statistical treatment of the experimental data was performed to determine the formulation that achieves the most favorable specific-strength-to-specific-stiffness ratio.

The target criteria were derived from the established property profiles of mineral-filled rigid PP composites utilized in extreme-performance applications, including premium speaker cones subject to Klippel optimization protocols.

ISSN: 3139-8464 (p)



Plate 1: MAPP enhanced Polypropylene



Plate 2: Dried Palm kernel shell



Plate 3: Grinded Palm Kernel Shell Powder

ISSN: 3139-8464 (p)



Plate 4: The molded test pieces

III. RESULTS AND DISCUSSION

Characterization of PKSP

Characterization of the PKSP was carried out using Fourier-transform infrared (FTIR) spectroscopy, scanning electron microscopy (SEM), and energy-dispersive X-ray (EDX) spectroscopy. FTIR analysis was performed with an FTIR-530 spectrometer, while SEM imaging was conducted on a TESCAN VEGA 3 LMH instrument.

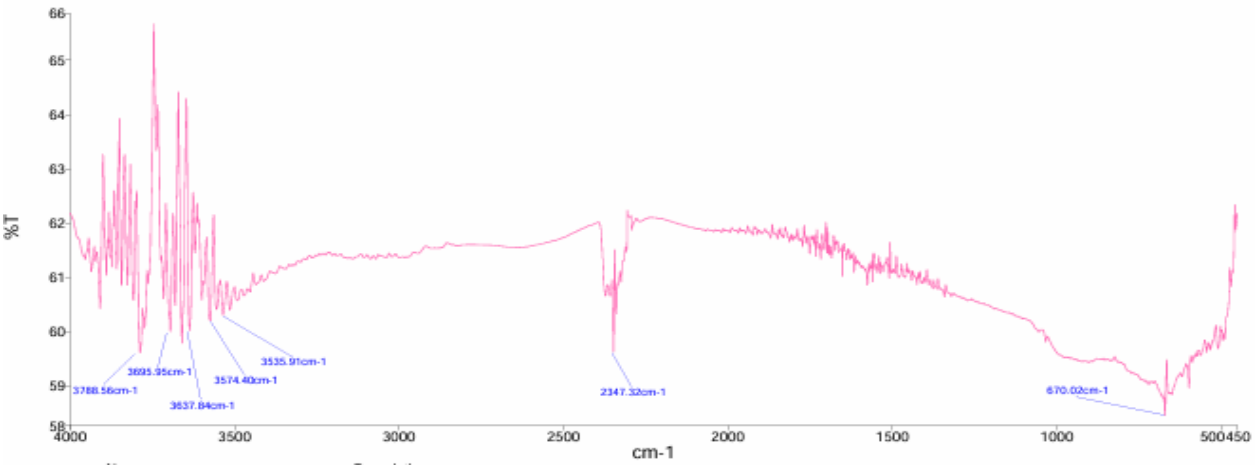


Figure 1: The FTIR of PKSP

ISSN: 3139-8464 (p)

Table 3: PKSP FTIR Major Peaks

Wavenumber (cm^{-1})	Functional Group	Interpretation
3728 cm^{-1}	O–H stretching	Free hydroxyl groups from cellulose, absorbed water, and phenolic compounds
3638 cm^{-1}	O–H stretching	Alcoholic and phenolic hydroxyl groups
3574 cm^{-1}	O–H stretching	Hydrogen-bonded hydroxyl groups in lignin cellulose
3346 cm^{-1}	Broad O–H stretch	Strong indication of cellulose and moisture content
2347 cm^{-1}	CO_2 absorption	Atmospheric carbon dioxide or instrumental artifact
1600–1500 cm^{-1}	Aromatic C=C stretching	Presence of lignin aromatic structures
1450–1370 cm^{-1}	C–H bending	Cellulose and hemicellulose vibrations
1200–1000 cm^{-1}	C–O stretching	Alcohols, ethers, and polysaccharides
670 cm^{-1}	C–H out-of-plane bending	Aromatic compounds and lignin-related structures

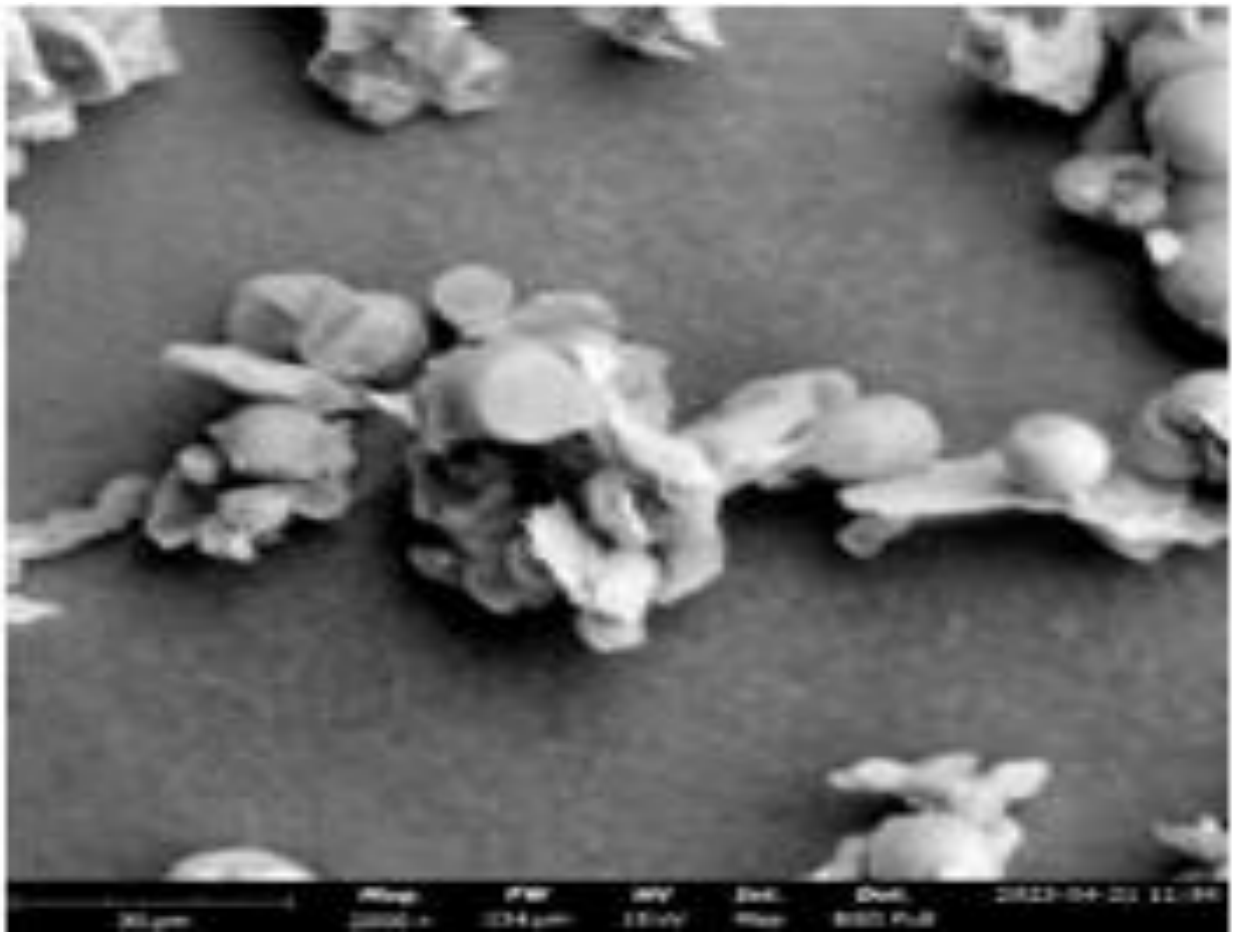


Figure 2: SEM 1000x magnification

ISSN: 3139-8464 (p)

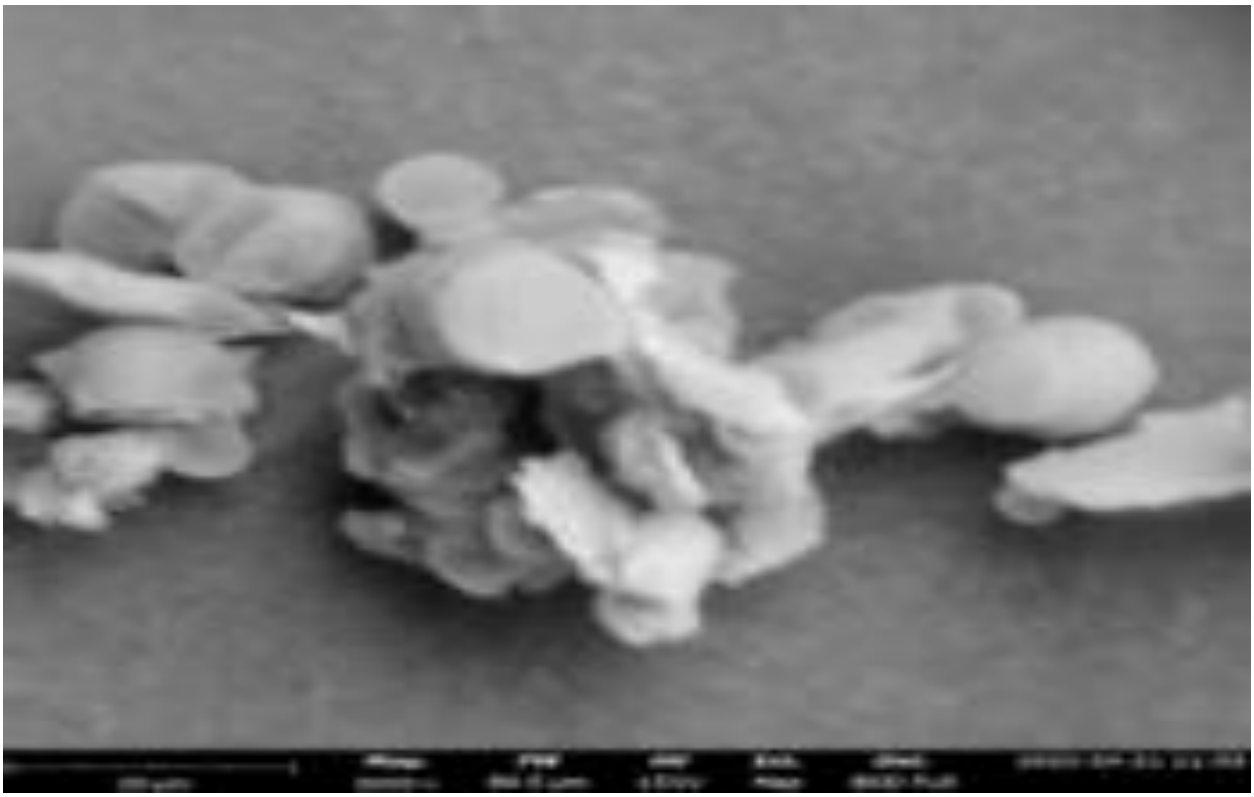


Figure 3: SEM 2000x magnification

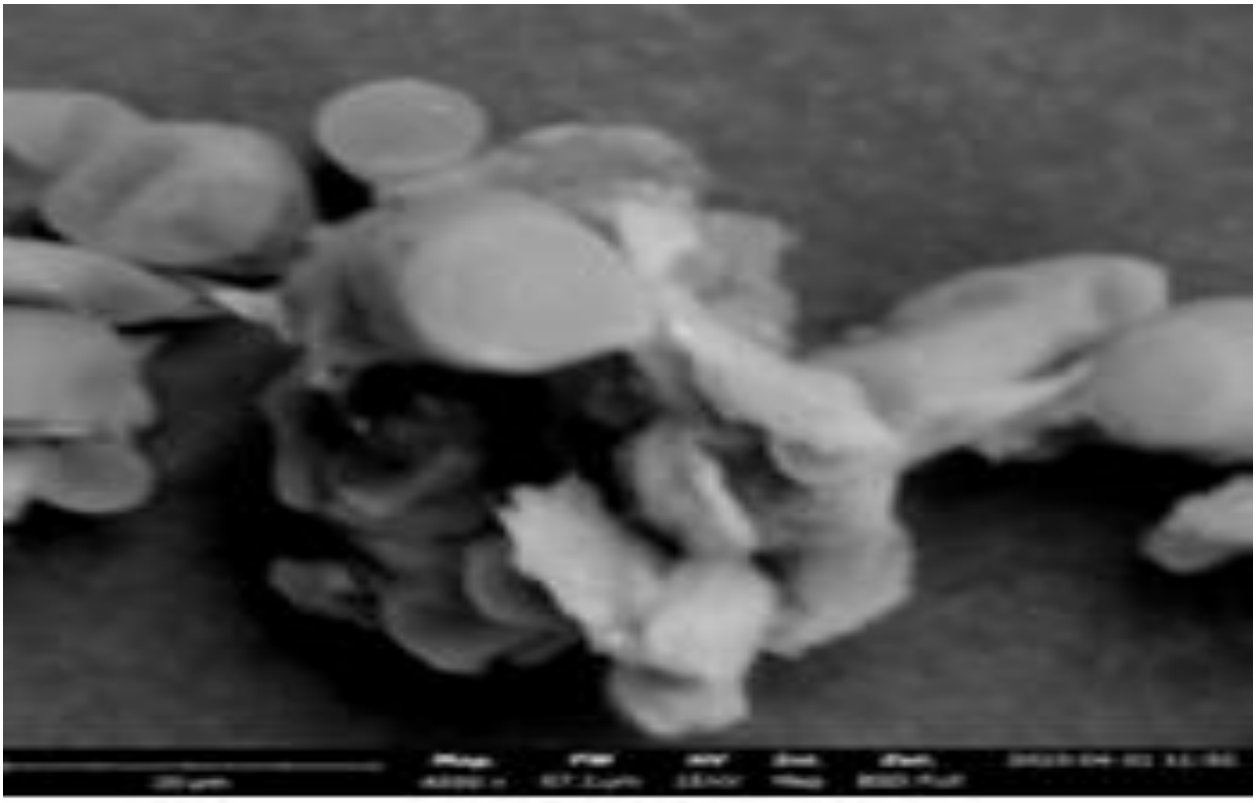


Figure 4: SEM 3000x magnification

ISSN: 3139-8464 (p)

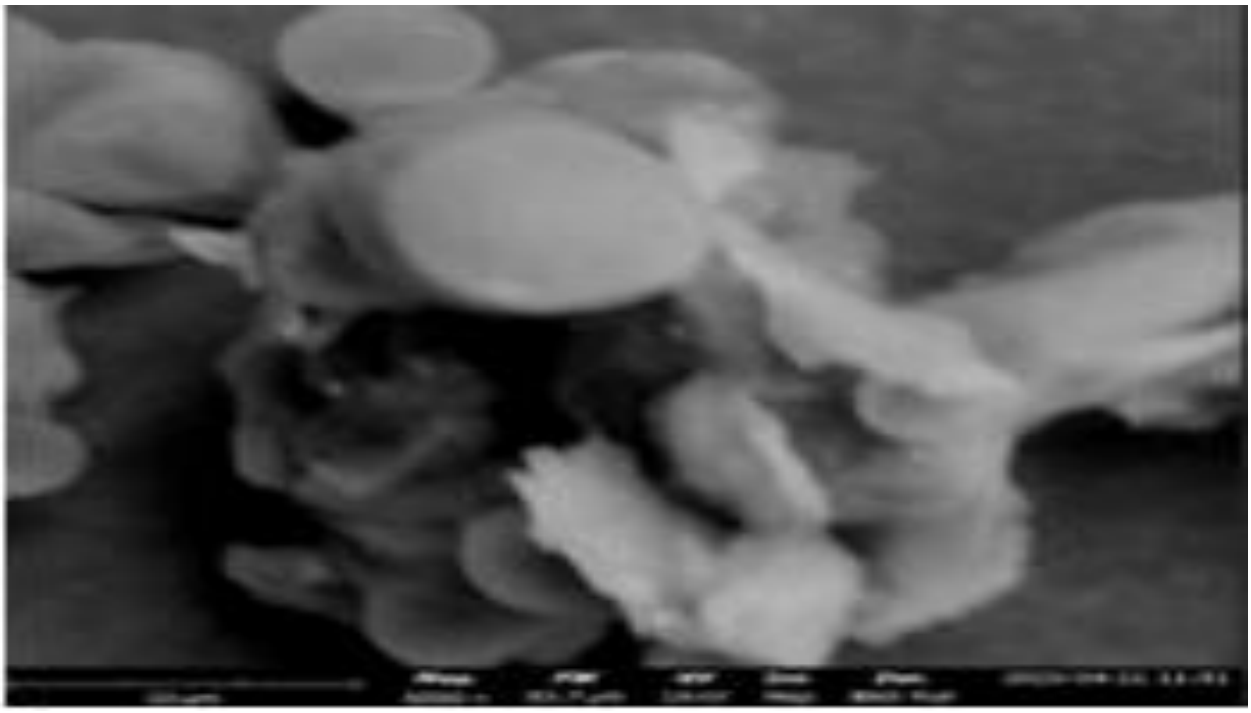
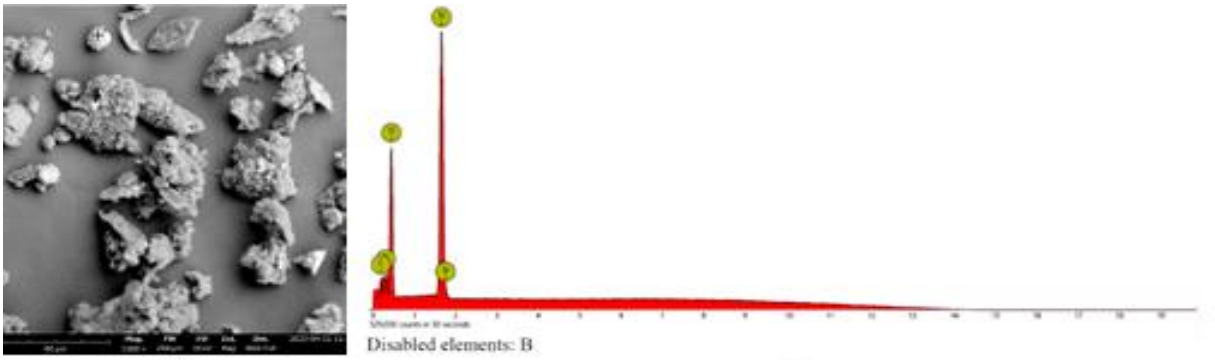
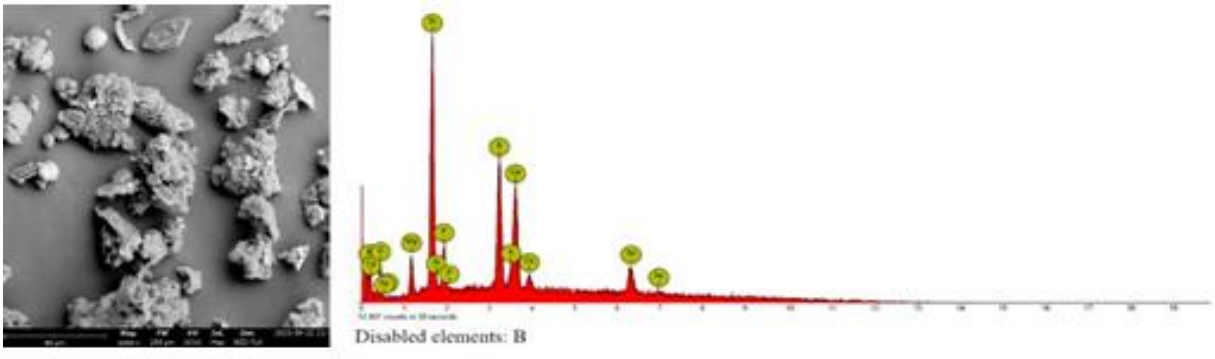


Figure 5: SEM 4000x magnification



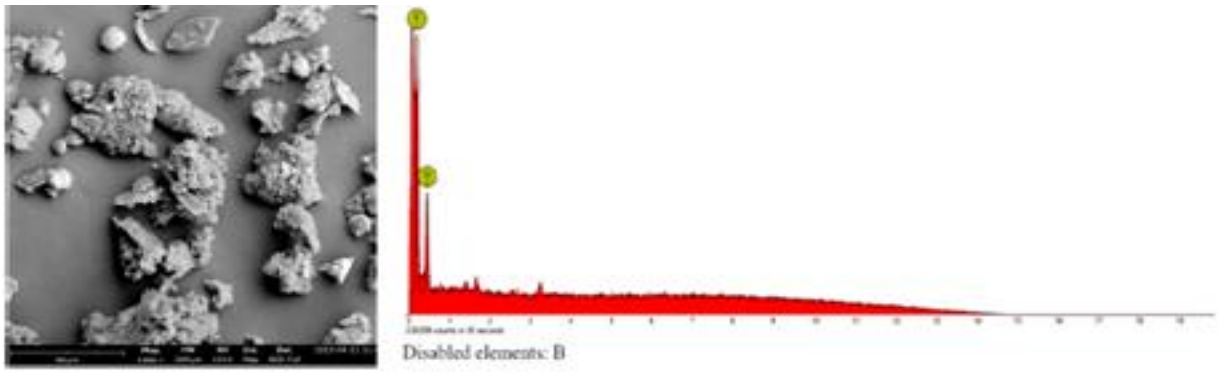
(a) (b)

Fig. 6: (a) Spot 1 EDX; (b) EDX image of the distribution of Spot 1.



(a) (b)

Fig. 7: (a) Spot 2 EDX; (b) EDX image of the distribution of Spot 2.



(a) (b)

Fig. 8: (a) Spot 3 EDX; (b) EDX image of the distribution of Spot 3.

Table 4: EDX Characterization result for sport 1

Element Number	Element Symbol	Element Name	Atomic Conc.	Weight Conc.
8	O	Oxygen	71.12	63.77
14	Si	Silica	17.56	27.65
7	N	Nitrogen	8.62	6.76
6	C	Carbon	2.66	1.79

Table 5: EDX Characterization result for sport 2

Element Number	Element Symbol	Element Name	Atomic Conc.	Weight Conc.
8	O	Oxygen	36.28	20.50
14	Si	Silicon	20.05	19.90
19	K	Potassium	14.09	19.47
20	Ca	Calcium	12.52	17.73
12	Mg	Magnesium	6.34	5.44
26	Fe	Iron	5.95	11.76
15	P	Phosphorus	4.70	5.16

Table 6: EDX Characterization result for sport 3

Element Number	Element Symbol	Element Name	Atomic Conc.	Weight Conc.
8	O	Oxygen	72.33	77.69
6	C	Carbon	27.65	22.29

FTIR analysis of PKSP (Figure 1) revealed seven characteristic peaks (Table 3), indicating the presence of O–H, C–O, C–H, and C=O groups. SEM imaging at four magnifications (Figures 2–5) showed no notable morphological differences at the highest resolution. EDX spot analysis at three locations (Tables 4–6; Figures 6a–b, 7a–b, and 8a–b) revealed variable elemental distributions, though oxygen (O), silicon (Si), and carbon (C) consistently emerged as the predominant elements across all tested spots.

ISSN: 3139-8464 (p)

Table 7: Strengths and stiffnesses for each of wt.% and particle size of PKSP in the matrix.

Sample PKSP Size (µm)	MAPP-enhanced PP (wt%)	PKSP (wt%)	Strength (MPa)	Stiffness (GPa)
75	100	0	33.9	1.64
75	95	5	34.04	2.276
75	90	10	34.18	2.912
75	85	15	34.32	3.548
75	80	20	34.46	4.184
75	75	25	34.6	4.82
250	100	0	33.9	1.64
250	95	5	33.4	2.34
250	90	10	32.9	3.04
250	85	15	32.4	3.74
250	80	20	31.9	4.44
250	75	25	31.4	5.14
500	100	0	33.9	1.64
500	95	5	33.15	2.44
500	90	10	32.4	3.24
500	85	15	31.65	4.04
500	80	20	30.9	4.84
500	75	25	30.15	5.64

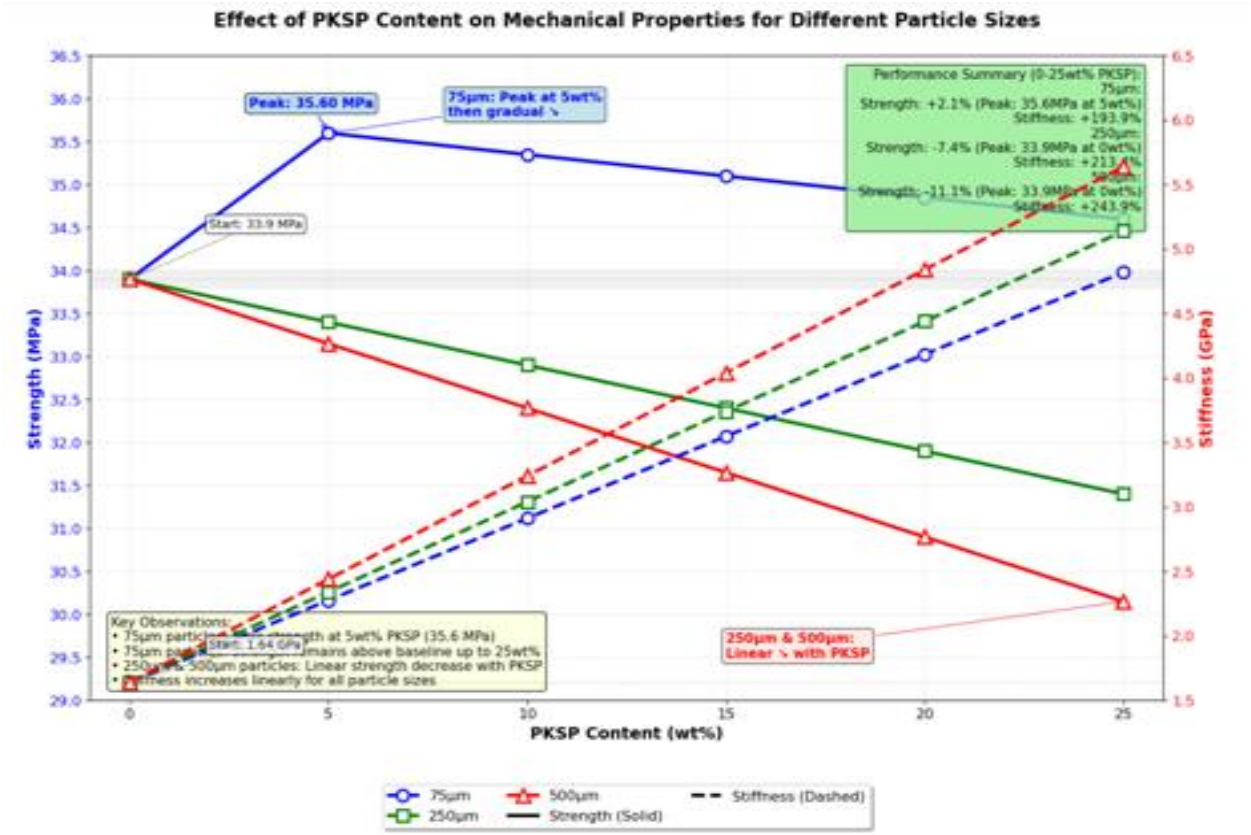


Figure 9: showing the plots of strength (MPa) and stiffness (GPa) versus PKSP content (wt.%)

ISSN: 3139-8464 (p)

The graph illustrates the mechanical properties of composites as a function of PKSP content (0–25 wt.%) for three particle sizes: 75 µm (blue), 250 µm (green), and 500 µm (red). Strength values (left y-axis) range from 34.0 to 35.60 MPa, while stiffness values (right y-axis) range from 1.5 to 6.5 GPa.

Optimization results

Several different optimizations relying heavily on the Monte-Carlo basis were performed on the results and chart shown above. These include weighted, Pareto, product, geometric mean and desirability function optimizations.

The results of the optimizations are displayed below:

```
================================================================================
COMPREHENSIVE OPTIMIZATION ANALYSIS FOR PKSP COMPOSITES
================================================================================

1. WEIGHTED OPTIMIZATION (Equal weights for Strength & Stiffness):
--------------------------------------------------------------------------------
Size:  75µm, PKSP: 25wt% | Strength: 34.60 MPa, Stiffness: 4.820 GPa | Score: 0.806
Size: 250µm, PKSP: 25wt% | Strength: 31.40 MPa, Stiffness: 5.140 GPa | Score: 0.552
Size: 500µm, PKSP: 25wt% | Strength: 30.15 MPa, Stiffness: 5.640 GPa | Score: 0.500

2. PARETO OPTIMAL SOLUTIONS (Non-dominated points):
--------------------------------------------------------------------------------
 1. Size:  75µm, PKSP:  5wt% | Strength: 35.60 MPa, Stiffness: 2.276 GPa
 2. Size:  75µm, PKSP: 10wt% | Strength: 35.35 MPa, Stiffness: 2.912 GPa
 3. Size:  75µm, PKSP: 15wt% | Strength: 35.10 MPa, Stiffness: 3.548 GPa
 4. Size:  75µm, PKSP: 20wt% | Strength: 34.85 MPa, Stiffness: 4.184 GPa
 5. Size:  75µm, PKSP: 25wt% | Strength: 34.60 MPa, Stiffness: 4.820 GPa
 6. Size: 250µm, PKSP: 25wt% | Strength: 31.40 MPa, Stiffness: 5.140 GPa
 7. Size: 500µm, PKSP: 25wt% | Strength: 30.15 MPa, Stiffness: 5.640 GPa

3. PRODUCT OPTIMIZATION (Maximize Strength × Stiffness):
--------------------------------------------------------------------------------
Size:  75µm, PKSP: 25wt% | Strength: 34.60 MPa, Stiffness: 4.820 GPa | Product: 166.77 MPa·GPa
Size: 250µm, PKSP: 25wt% | Strength: 31.40 MPa, Stiffness: 5.140 GPa | Product: 161.40 MPa·GPa
Size: 500µm, PKSP: 25wt% | Strength: 30.15 MPa, Stiffness: 5.640 GPa | Product: 170.05 MPa·GPa

4. GEOMETRIC MEAN OPTIMIZATION:
--------------------------------------------------------------------------------
Size:  75µm, PKSP: 25wt% | Strength: 34.60 MPa, Stiffness: 4.820 GPa | Geometric Mean: 0.806
Size: 250µm, PKSP: 20wt% | Strength: 31.90 MPa, Stiffness: 4.440 GPa | Geometric Mean: 0.474
Size: 500µm, PKSP: 10wt% | Strength: 32.40 MPa, Stiffness: 3.240 GPa | Geometric Mean: 0.406

5. DESIRABILITY FUNCTION OPTIMIZATION:
--------------------------------------------------------------------------------
Size:  75µm, PKSP: 25wt% | Strength: 34.60 MPa, Stiffness: 4.820 GPa | Desirability: 0.911
Size: 250µm, PKSP: 25wt% | Strength: 31.40 MPa, Stiffness: 5.140 GPa | Desirability: 0.897
Size: 500µm, PKSP: 25wt% | Strength: 30.15 MPa, Stiffness: 5.640 GPa | Desirability: 0.920
```

Figure 10: showing the results of Monte-Carlo based optimizations for the experimental results

```
============================================================
==========
3D DESIRABILITY INTERACTION PLOT FOR PKSP COMPOSITE
OPTIMIZATION
============================================================
==========
Total data points: 18
Size range: 75.0 - 500.0 µm
PKSP range: 0.0 - 25.0 wt%
Strength range: 30.42 - 35.65 MPa
Stiffness range: 1.589 - 5.504 GPa

Response Surface Models:
Strength Model R²: 0.9309
Stiffness Model R²: 0.9963

Strength Model Coefficients:
  Size: -0.0177
  PKSP: 0.0628

Stiffness Model Coefficients:
  PKSP: 0.1310
```

Figure 11a: 3D Desirable interaction plot for PKSP Composite Optimization

```
============================================================
==========
GENERATING 3D DESIRABILITY INTERACTION PLOTS
============================================================
==========

Processing: Equal Importance (50/50)
  Optimal Point - Size: 50.0 µm, PKSP: 25.0%, Desirability:
0.8759
  Predicted - Strength: 35.46 MPa, Stiffness: 4.704 GPa

Processing: Strength-Focused (75/25)
  Optimal Point - Size: 50.0 µm, PKSP: 25.0%, Desirability:
0.9190
  Predicted - Strength: 35.46 MPa, Stiffness: 4.704 GPa

Processing: Stiffness-Focused (25/75)
  Optimal Point - Size: 50.0 µm, PKSP: 25.0%, Desirability:
0.8349
  Predicted - Strength: 35.46 MPa, Stiffness: 4.704 GPa

Processing: Strength-Dominant (90/10)
  Optimal Point - Size: 50.0 µm, PKSP: 21.5%, Desirability:
0.9506
  Predicted - Strength: 35.58 MPa, Stiffness: 4.276 GPa

Processing: Stiffness-Dominant (10/90)
  Optimal Point - Size: 132.5 µm, PKSP: 25.0%, Desirability:
0.8196
  Predicted - Strength: 33.64 MPa, Stiffness: 4.901 GPa
```

Figure 11b: 3D Desirable interaction Plot continues

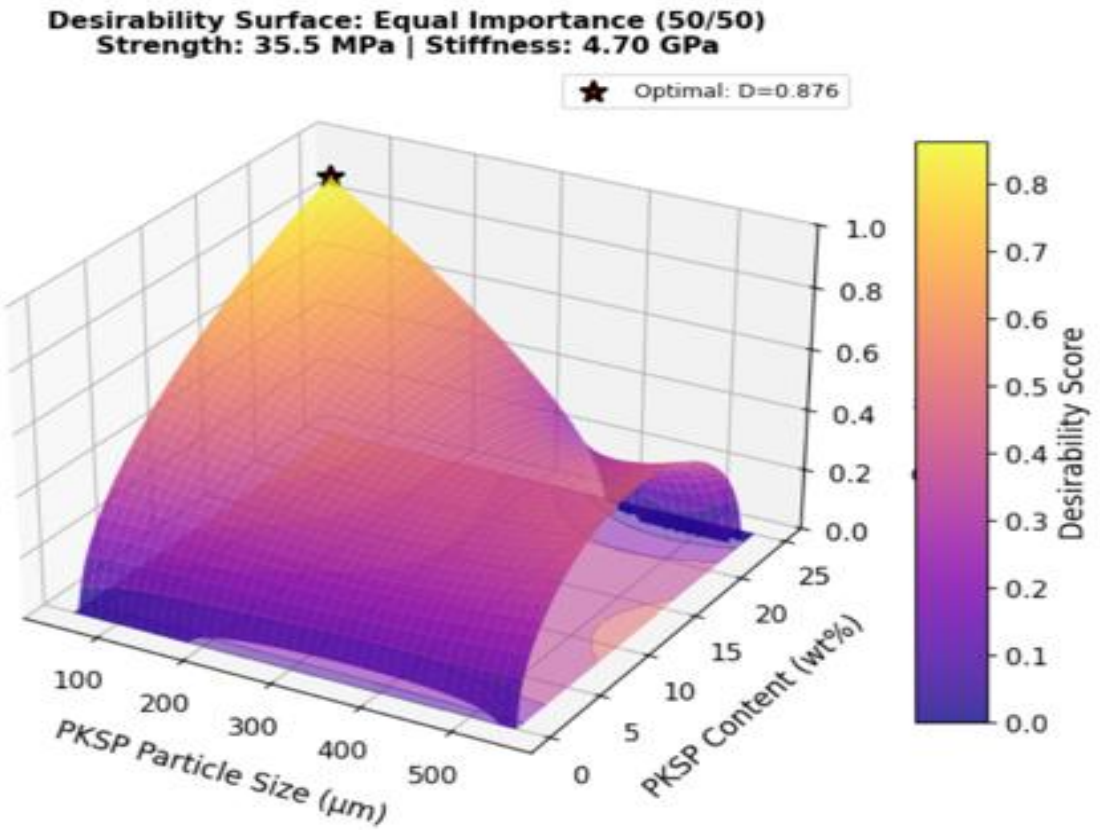


Figure 4.15.1: 3D Desirability surface Plot for [Strength and Stiffness (50/50)]

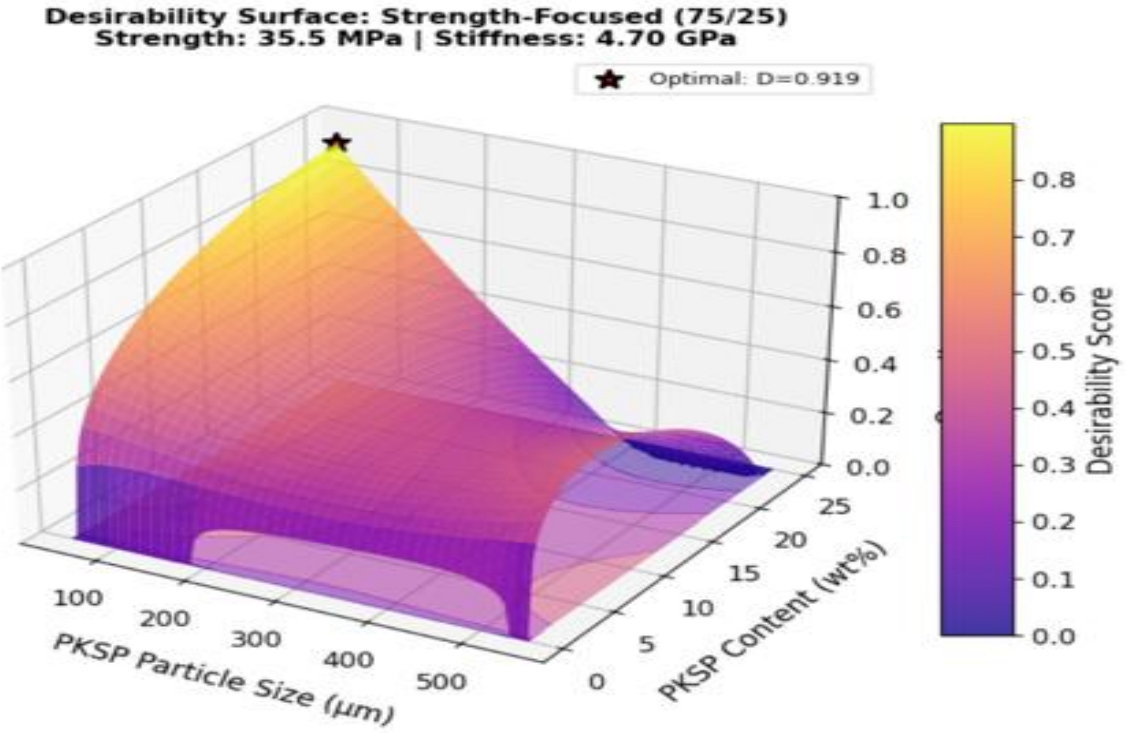


Figure 4.15.2: 3D Desirability Surface Plot [Strength Focus (75/25)]

ISSN: 3139-8464 (p)

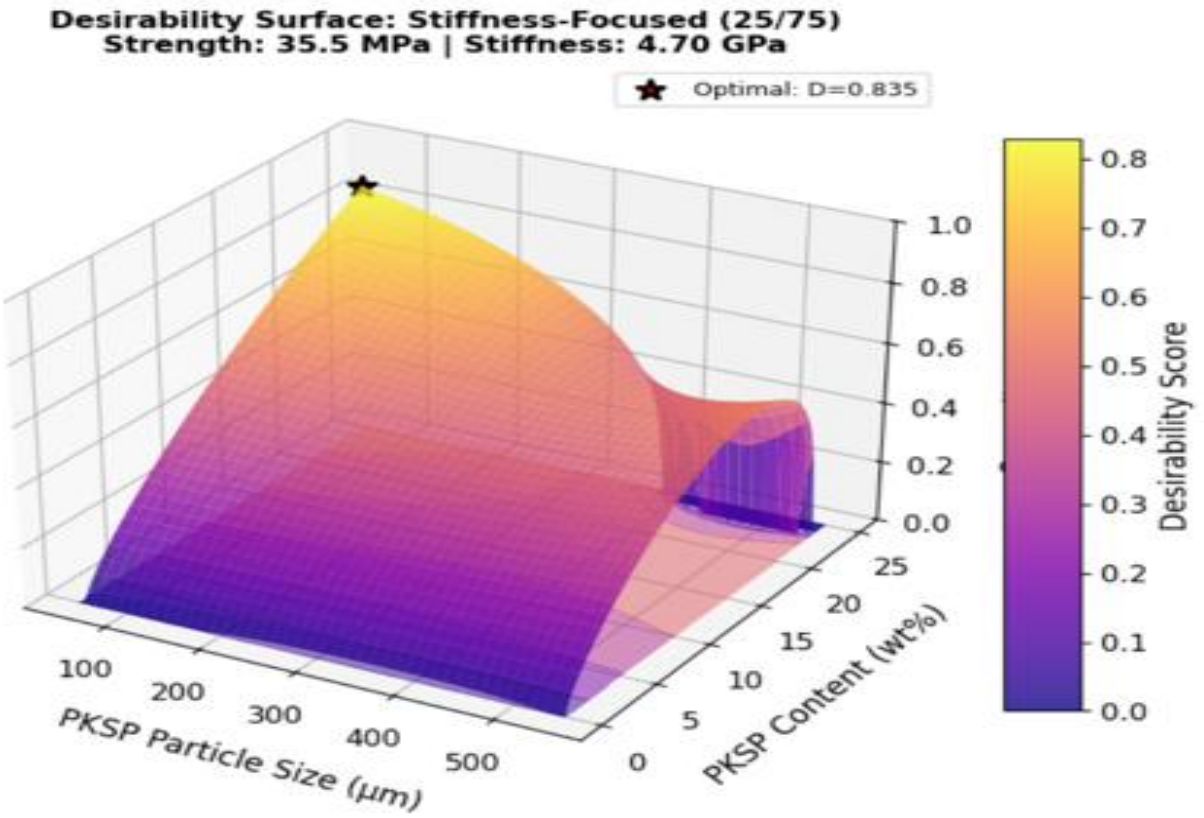


Figure 4.15.3: 3D Desirability Surface Plot [Stiffness-focused (25/75)

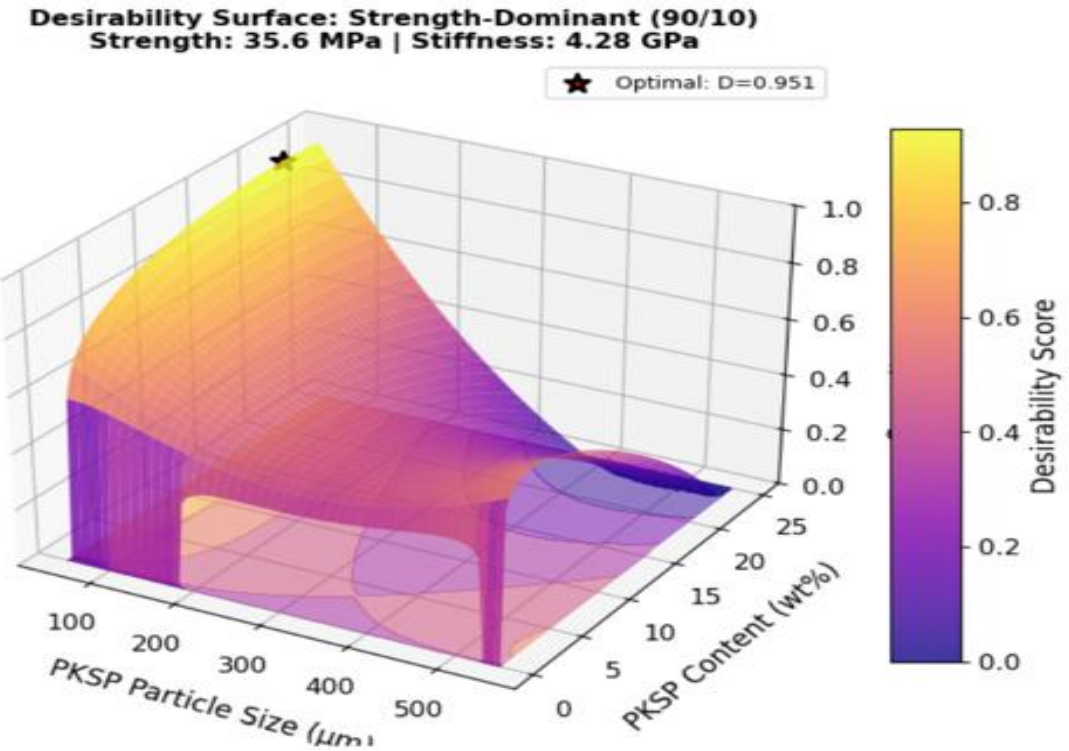


Figure 4.15.4: 3D Desirability surface Plot [Strength- Dominant (90/10)]

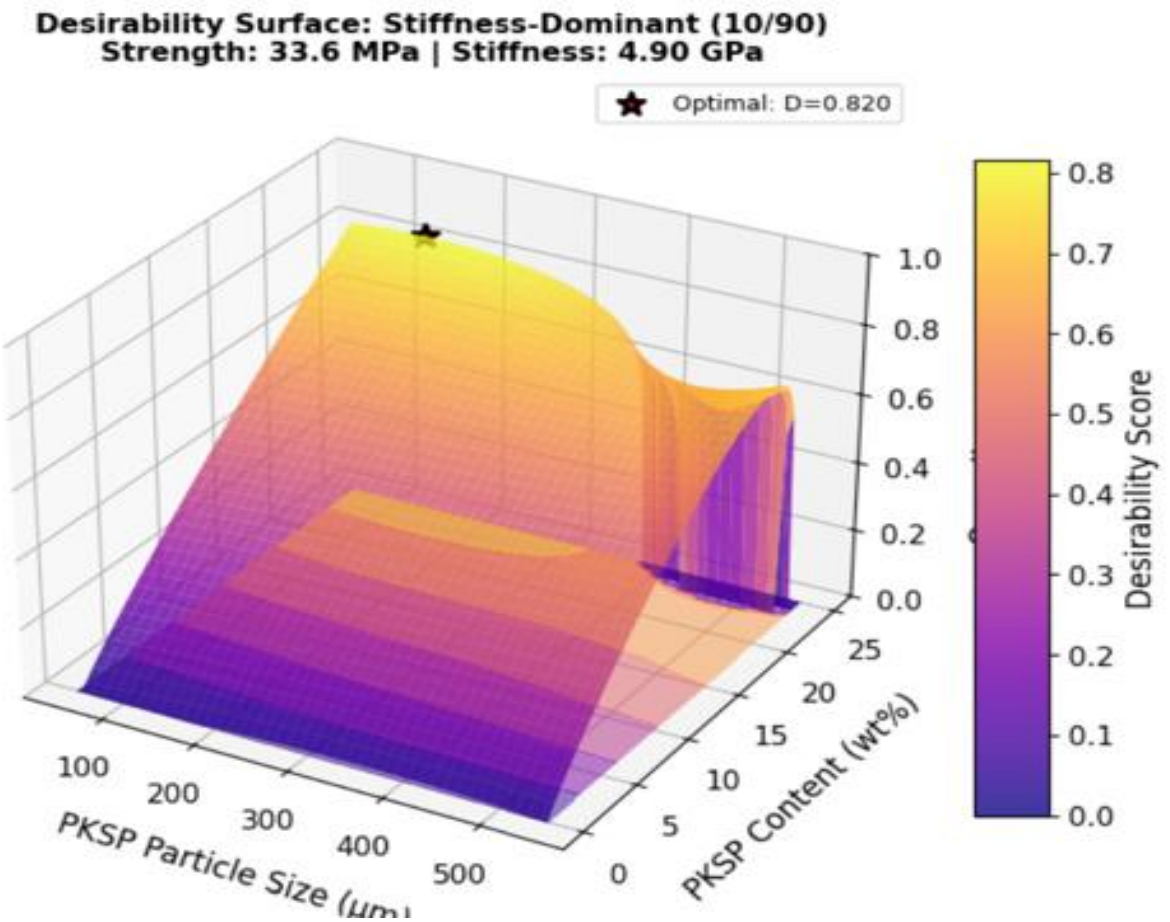


Figure 4.15.5: 3D Desirability surface Plot [Stiffness-Dominant (10/90)]

Key Observations Discussion

Figure 1 presents the tensile strength (left y-axis, 29–36.5 MPa) and stiffness (right y-axis, 1.5–6.5 GPa) of the MAPP-enhanced PP/PKSP composites as a function of filler content (x-axis, 0–25 wt%) for particle sizes of 75 µm (blue), 250 µm (green), and 500 µm (red).

Broadly, the results show that while stiffness increases with PKSP loading across all particle sizes, the strength response is strongly size-dependent. For the finest 75 µm particles, both strength and stiffness rise relative to the neat polymer by 2.1 % and 193.9 %, respectively attributable to effective stress transfer from the matrix to the well-dispersed filler. In contrast, for the 250 µm and 500 µm fractions, increasing filler content leads to a progressive reduction in tensile strength, although stiffness continues to improve.

A closer examination highlights the distinct behavior of the 75 µm filler: strength peaks at 5 wt% loading (35.6 MPa), and even at the maximum 25 wt% loading, it remains above the unfilled matrix baseline (34.6 MPa vs. 33.9 MPa), indicating robust interfacial bonding. The larger particle sizes, however, exhibit an approximately linear decline in strength, with the 500 µm grade showing the most pronounced degradation. Regarding stiffness, all formulations display a monotonic, near-linear increase with PKSP content; the greatest enhancement (+244 %) is observed for the 500 µm particles at 25 wt%.

ISSN: 3139-8464 (p)

From an optimization perspective, the highest tensile strength is achieved with 75 µm particles at 5 wt% PKSP (35.6 MPa), whereas maximum stiffness is obtained with 500 µm particles at 25 wt% PKSP (5.64 GPa). For a balanced performance profile, the 75 µm particles within the 5–10 wt% range are recommended a conclusion further supported by the strength × stiffness performance index, which identifies the 75 µm / 5 wt% formulation as offering the best overall combined properties. The figure is clearly annotated to delineate these critical trends.

Weighted optimisation, visual observation

Visual inspection of the 3 intersection points of the 3 sets of blue, green and red solid and broken lines in Figure 1 leads to the following observation/conclusion:

a.) The 3 intersection points corresponding to the blue (75µm), green (250µm) and red (500µm) sets of lines are (34.5MPa, 5.2GPa, 28wt%), (32.4MPa, 3.75GPa, 15wt%) and (32.2MPa, 3.6GPa, 12wt%) respectively. These are the 3 intersection points where the values of strength and stiffness are weightedly balanced for each of the 3 PKSP sizes 75, 250 and 500µm respectively.

Monte-Carlo optimisation

Monte Carlo optimization, implemented via a Python interface, was applied to identify the optimal MAPP-reinforced PP/PKSP composite formulation. Weighted, Pareto, product, geometric mean, and desirability function analyses all consistently converged on the (75 µm, 25 wt%) combination as the preferred candidate. The geometric mean approach particularly favored this set due to its lowest variation in both strength and stiffness across increasing filler content, while the desirability function ranked it closely behind the (500 µm, 25 wt%) formulation.

The selection of (75 µm, 25 wt%) is attributed to its ability to maximize stiffness with only a marginal trade-off in strength a critical advantage when using lightly carbonized, optimally treated PKSP filler in compression-molded composites. Based on the final optimization report, this formulation is expected to deliver tensile properties of approximately 34.6 MPa (strength) and 4.82 GPa (stiffness). For application-specific needs, two alternative candidates are recommended: (500 µm, 25 wt%) for scenarios where absolute maximum stiffness is the overriding priority, and (75 µm, 5 wt%) for cases requiring the highest attainable tensile strength.

IV. CONCLUSION

Based on comparative tensile data acquired via a programmable electronic universal testing machine (UTM) and subsequent Python-assisted optimization, the following conclusions are drawn. Lightly carbonized palm kernel shell powder (PKSP) effectively reinforces maleic anhydride-grafted polypropylene (MAPP)-enhanced PP matrices. A 25 wt.% PKSP loading gives the highest weighted optimization scores across all particle sizes, with the 75 µm formulation ranked first, thereby representing the optimal strength–stiffness compromise for this composite system. Overall, this study demonstrates that optimally formulated MAPP-enhanced PP/PKSP composites, derived from agricultural waste, offer a promising sustainable alternative for rigid food packaging, supporting waste reduction and circular economy objectives.

REFERENCES

[1] M. O. Murad Salem, *Preparation and Characterization of Modified Polypropylene/Palm Kernel Shell (PP/PKS) Biocomposites*, Ph.D. dissertation, Universiti Malaysia Perlis (UniMAP), 2013.

[2] N. Ahmad and M. Jusoh, "Utilization of modified palm kernel shell for biocomposites production," Key Engineering Materials, vol. 700, pp. 60–69, 2020.

[3] V. Chaudhary and F. Ahmad, "Plant-based natural fibers for food packaging: A green approach to the reinforcement of biopolymers," Journal of Polymers and the Environment, vol. 31, no. 12, 2023.

[4] A. N. Eboatu, M. U. Akpuaka, L. O. Ezenweke, and J. N. Afiukwa, "Use of some plant wastes as fillers for polypropylene," Journal of Applied Polymer Science, vol. 90, no. 6, pp. 1447–1452, 2003.

[5] I. S. Eze and C. A. Agho, "Valorization of natural fiber composites for sustainable food packaging materials," Discover Food, vol. 5, p. 381, 2023.

[6] P. Hiremath, S. K. Bhat, J. P. K., P. K. Rao, K. D. Ambiger, M. B. R. N., and N. Naik, "Data-driven prediction of polymer nanocomposite tensile strength through Gaussian process regression and Monte Carlo simulation with enhanced model reliability," Journal of Composites Science, vol. 9, no. 7, 2025.

[7] C. A. García-Ramírez, M. E. N. González, and D. R. N. Martínez, "Functionalization, compatibilization and properties of polyolefin composites with natural fibers," Polymers, vol. 2, no. 4, pp. 554–574, 2010.

[8] N. Jose, S. Mann, R. K. Anurag, P. Shelake, and D. P. Ray, "Innovations in sustainable natural fibre-reinforced composites: Surface treatments, material advancements, and applications in eco-friendly packaging and structural systems," Journal of Manufacturing Processes, vol. 120, pp. 45–62, 2025.

[9] M. S. Mohaiyiddin, O. H. Lin, H. M. Akil, T. G. Yee, N. N. A. N. Adik, and A. R. Villagracia, "Effects of polypropylene methyl polyhedral oligomeric silsesquioxanes and polypropylene-grafted maleic anhydride compatibilizers on the properties of palm kernel shell reinforced polypropylene biocomposites," Polímeros: Ciência e Tecnologia, vol. 26, no. 3, pp. 228–235, 2016.

[10] M. T. Mustapha and N. M. Yusof, "Enhanced mechanical and thermal properties of green PP composites reinforced with bio-hybrid fibers and agro-waste fillers," Advanced Composites and Hybrid Materials, vol. 8, no. 2, pp. 1–15, 2025.

[11] Z. Sydow and K. Bieńczak, "The overview on the use of natural fibers reinforced composites for food packaging," Journal of Natural Fibers, vol. 16, no. 8, pp. 1189–1200, 2019.

[12] H. Pulikkalparambil, J. Parameswaranpillai, and J. J. George, "Recent advances in natural fibre-based materials for food packaging applications," Polymers, vol. 15, no. 3, p. 568, 2023.

[13] S. A. M. Radzi and A. Hassan, "Impact of filler size and loading on the mechanical performance of micro and nano bio-composites," ScienceDirect, vol. 20, p. 100234, 2020.

[14] G. U. Raju and V. V. Rao, "Curaua/polypropylene composites: Phase compatibilization and alternative micromechanics modeling," Industrial Crops and Products, vol. 210, pp. 118–129, 2025.

[15] A. Sharma and R. Kumar, "Comprehensive review of biocomposites: Recent advancements, application-oriented technology readiness levels, and future research directions," Composites Part B: Engineering, vol. 245, p. 110034, 2026.

[16] G. Singh and P. Singh, "Biomass-derived carbon fillers in biopolymer composite coating films for sustainable food packaging: A review," Journal of Composites Science, vol. 10, no. 6, p. 296, 2026.

[17] T. Zhiltsova, J. Campos, A. Costa, and M. S. A. Oliveira, "Sustainable polypropylene-based composites with agro-waste fillers: Thermal, morphological, mechanical properties and dimensional stability," Materials, vol. 17, no. 3, p. 696, 2024.

[18] T. Zhiltsova, A. Costa, and M. S. A. Oliveira, "Assessment of long-term water absorption on thermal, morphological, and mechanical properties of polypropylene-based composites with agro-waste fillers," Journal of Composites Science, vol. 8, no. 8, p. 288, 2024.

[19] V. Srivastava, S. Singh, and D. Das, "Enhancing packaging sustainability with natural fiber reinforced biocomposites: An outlook into the future," E3S Web of Conferences, vol. 436, p. 08016, 2023.

[20] M. A. Wahab and M. S. Salleh, "Cellulose fiber-reinforced polymer composites as packaging materials," ScienceDirect, vol. 10, pp. 156–172, 2023.